

# ChartAct: A Benchmark for Dynamic Chart Understanding

Muye Huang<sup>1,2,\*</sup>, Lin Wu<sup>1,2,\*</sup>, Lingling Zhang<sup>1,2,†</sup>, Hang Yan<sup>1,2</sup>, Zhiyuan Wang<sup>1,2</sup>,  
Yumeng Fu<sup>1,2</sup>, Zesheng Yang<sup>1,2</sup>, Jun Liu<sup>1,2</sup>

<sup>1</sup>School of Computer Science and Technology, Xi'an Jiaotong University

<sup>2</sup>MOE KLNN Lab, Xi'an Jiaotong University

{huangmuye, wl19503611685, shihanghanya233, 2444821229}@stu.xjtu.edu.cn

{yumfuu, youngzsh}@stu.xjtu.edu.cn, {zhanglling, liukeen}@xjtu.edu.cn

\*Equal contribution. †Corresponding author.

## Abstract

Charts are widely used to present complex data for analysis and decision making. Existing chart understanding benchmarks mainly focus on static charts, but real-world charts are often dynamic and interactive. Key information may only appear after actions such as hovering, clicking, zooming, or dragging. Dynamic chart understanding therefore requires models to identify visible content, choose proper interactions, and reason over changing chart states. To evaluate this ability, we propose ChartAct, an interactive benchmark for dynamic chart understanding. ChartAct collects and filters 673 dynamic charts from 8 real chart websites, covers 7 common chart types, and constructs 1,440 high-quality question-answer samples. Each sample is instantiated in two environments, Dynamic Chart and Dashboard Chart, to evaluate dynamic chart understanding under different contexts. Based on ChartAct, we systematically evaluate 11 advanced multimodal models and GUI agents. Experimental results show that existing models still have clear limitations in dynamic chart understanding. The strongest model, Claude-Opus-4.7, achieves an average success rate of 84.5%, while most models remain below 60%. We also conduct detailed failure attribution and case analysis. ChartAct provides a new benchmark for studying chart understanding in real interactive environments. Codes at [https://github.com/wulin-wulin/OSWorld\\_Chart](https://github.com/wulin-wulin/OSWorld_Chart)

## 1 Introduction

Charts are a widely used form of data visualization, capable of presenting complex data relationships in an intuitive manner. Charts commonly appear in scientific papers, business reports, financial analysis, and public data platforms. Automated chart

understanding is an important step toward automated data analysis. This task requires models to understand axes, legends, text, colors, shapes, and data points in charts, and further perform a series of complex inferences. In recent years, extensive chart understanding benchmarks (Methani et al., 2020; Kafle et al., 2018; Chaudhry et al., 2020; Kahou et al., 2018; Masry et al., 2025) have driven substantial progress of MLLMs (Bai et al., 2023; Wang et al., 2024a; Masry et al., 2024b; Li et al., 2024; Yang et al., 2023) in chart understanding.

However, existing chart evaluation benchmarks focus on static charts, where all information is presented through a static image. This setting does not fully match the form of charts in real scenarios. Charts in real scenarios usually have dynamic and interactive properties, which we refer to as dynamic charts. A large number of dynamic charts are embedded in webpages or dashboards, where users need to interact with the interface to obtain the required information. When analyzing charts, users may hover over data points to inspect precise values, click legends to switch data series, or drag time sliders to observe changes across different stages. In these scenarios, key information is often not fully available in the initial chart state. Models need to obtain new information through interface actions and complete reasoning based on continuously changing chart states.

This process imposes higher requirements on chart understanding. First, models need the ability to interact with chart environments. The evidence required by real questions often needs to be obtained progressively through actions, so models must select appropriate interactions according to the question and update the subsequent reasoning process based on new observations. Second,



Figure 1: Illustration of dynamic chart understanding in ChartAct. The model starts from the initial chart state, performs actions such as zooming and hovering to reveal hidden evidence, and answers the question based on the newly observed chart state.

models need to precisely understand and locate visual elements and interactive elements in dynamic charts. Markers, controls, and interface states in dynamic charts jointly determine the currently visible information. If a model cannot accurately locate target elements or understand their functions, it is difficult to perform effective interactions. Existing static chart evaluations mainly focus on visible information in a single image, and thus cannot adequately evaluate interaction decision-making, element localization, and evidence acquisition in dynamic chart environments.

To study this problem, we propose ChartAct, a benchmark for dynamic chart understanding. ChartAct places dynamic charts in interactive environments, allowing models to change chart states through actions, as Figure 1 shows. Changes in chart states produce new observable information, which provides evidence for the model’s subsequent reasoning. This process is close to real dynamic chart analysis. When analyzing dynamic charts, users usually operate the chart repeatedly according to the question, observe the feedback, and update their judgments. ChartAct evaluates the dynamic chart understanding ability of models around this process. To support this evaluation, we need to construct an evaluation environment that preserves both the complexity of real charts and

the controllability of interaction processes.

Specifically, we crawl 673 dynamic charts from 8 real websites, and manually filter the collected charts to retain samples with clear data semantics, rich interactive behaviors, and high analytical value. We further embed these dynamic charts into controllable interactive environments, constructing interactive evaluation environments that contain charts, titles, controls, and other components. Based on these environments, we design tasks covering visible-state question answering, interaction-revealed information, cross-state comparison, multi-chart evidence integration, and interactive context understanding. We evaluate current advanced multimodal models and GUI agents (Nguyen et al., 2025) on ChartAct, and analyze their failure modes in chart localization, action selection, state observation, and evidence integration.

Our main contributions are summarized as follows:

- We propose ChartAct, a benchmark for dynamic chart understanding, which evaluates the ability of models to acquire chart evidence through actions and complete reasoning in interactive environments.
- We construct an evaluation set based on dynamic charts from real websites. We manu-

ally filter high-value chart samples and embed them into controllable simulated dashboards, preserving both real chart complexity and reproducible interactive environments.

- We systematically evaluate advanced multi-modal models and GUI agents, revealing key limitations of current models in chart localization, interaction action selection, state observation, and cross-state evidence integration.

## 2 Related Work

### 2.1 Chart Understanding Datasets

Chart understanding datasets are the basis for evaluating chart perception and reasoning. Early benchmarks such as FigureQA (Kahou et al., 2018), DVQA (Kafle et al., 2018), and PlotQA (Methani et al., 2020) mainly use synthetic charts and template-based questions. Later datasets, including ChartQA (Masry et al., 2022, 2025), RealCQA (Ahmed et al., 2023), ChartX (Xia et al., 2024), UniChart (Masry et al., 2023), expand chart sources and training data. ChartQA introduces real charts and human-written questions, while UniChart provide larger-scale data by integrating existing datasets or generating new samples. Recent benchmarks such as CharXiv (Wang et al., 2024b) and EvoChart (Huang et al., 2025) further move chart evaluation toward real world scenario charts. DashboardQA (Kartha et al., 2026) focus on dashboards. Most existing datasets still focus on static charts. ChartAct extends this direction to dynamic charts, where models need interaction to acquire chart evidence.

### 2.2 MLLMs for Chart Understanding

MLLMs have become a major approach for chart understanding. Earlier methods such as DePlot (Liu et al., 2023a), MatCha (Liu et al., 2023b), UniChart (Masry et al., 2023), and ChartReader (Cheng et al., 2023) improve chart question answering through chart parsing or chart-specific pre-training. Recent methods, including ChartLlama (Han et al., 2023), ChartAssistant (Meng et al., 2024), ChartInstruct (Masry et al., 2024a), TinyChart (Zhang et al., 2024), and ChartMoE (Xu et al., 2025), use chart instruction data and specialized architectures to improve chart perception and reasoning. General MLLMs (Chen et al., 2023; Team et al., 2025; Team, 2024; Bai et al., 2025; Abidin et al., 2024) also achieve strong results on static chart benchmarks such as ChartQA. These methods

mainly answer from a single chart image. ChartAct evaluates models in dynamic chart environments, where models must observe state changes and reason from interactively acquired evidence.

### 2.3 GUI Agents

GUI agents operate graphical interfaces through visual perception, grounding, and sequential actions. Recent benchmarks and systems (Liu et al., 2026; Yang et al., 2026; Chen et al., 2025; Gou et al., 2025), such as OSWorld and Mobile-Agent-v3 (Xie et al., 2024; Ye et al., 2025), evaluate agents in executable desktop or mobile environments and study their abilities in interface grounding, planning, and environment feedback. These works show strong progress in general GUI automation, but they mainly focus on broad application-level tasks. ChartAct studies a more focused setting, where agents must control the interface to reveal chart evidence and then reason over visual data. This setting connects GUI interaction with chart understanding.

## 3 ChartAct Benchmark

We propose ChartAct, an interactive evaluation benchmark for dynamic chart understanding. ChartAct centers on real dynamic charts, places them in controllable interactive environments, and requires models to answer chart questions through actions, observations, and reasoning. Each sample consists of a dynamic chart, an interactive environment, a question, and a ground-truth answer. A model starts from the initial chart state, selects interaction actions according to the question, and observes new visible information after the chart state changes. It provides evidence for subsequent reasoning. Based on this process, ChartAct evaluates models’ interaction decision-making, state observation, and evidence integration abilities in dynamic charts.

### 3.1 Data Construction

**Chart collection.** We collect dynamic charts with interactive functions from real websites. To ensure that the charts are suitable for interactive evaluation, we manually filter the candidate charts. The filtering process mainly removes two types of samples. The first type contains charts with weak interactivity. These charts may include animations or visual changes, but the changes mainly occur at the visual presentation level. Their chart content does not change effectively through interaction,

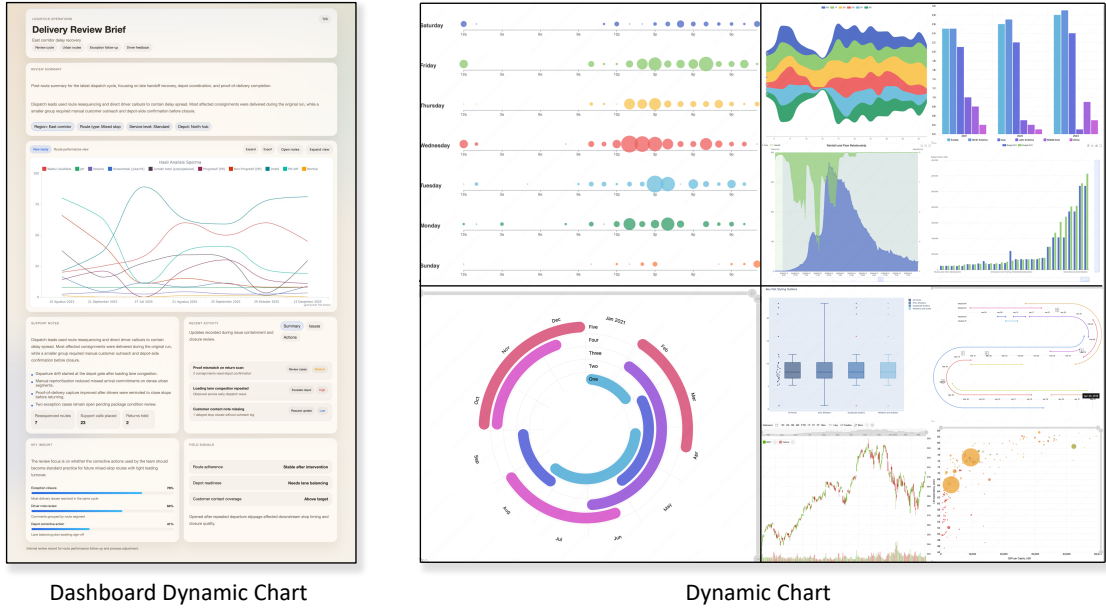


Figure 2: Examples of the two evaluation environments in ChartAct. Dashboard Chart embeds a dynamic chart into a dashboard page, while Dynamic Chart presents the same type of interactive chart in a clean chart environment.

Source	Line	Bar	Bubble	Pie	Heatmap	Box	Other	Total
Apache ECharts	13	13	13	13	13	13	4	82
VChart	13	13	13	13	2	3	4	61
Highcharts	13	18	8	11	7	2	13	72
AnyChart	16	18	15	15	9	20	8	101
Chart.js	40	10	6	8	0	0	4	68
amCharts	16	18	11	14	8	0	18	85
Plotly	17	19	17	11	12	19	14	109
AntV G2	19	19	19	19	9	10	0	95
<b>Total</b>	<b>147</b>	<b>128</b>	<b>102</b>	<b>104</b>	<b>60</b>	<b>67</b>	<b>65</b>	<b>673</b>

Table 1: Distribution of collected interactive charts across sources and chart types.

and the interaction process does not provide new data evidence. The second type contains charts that are unsuitable for interactive tasks. These charts may change continuously and lack a stable observable state, making it difficult for models to observe, operate, and answer under a clear state. After filtering, we retain 673 interactive charts from 8 real websites. These charts cover 7 types, including line charts, bar charts, scatter/bubble charts, pie/donut charts, heatmaps, box/candlestick charts, and other charts. The chart types are kept relatively balanced within the range of collectable samples.

**Question construction.** After obtaining the filtered dynamic charts, we construct candidate question-answer pairs for each chart. We use GPT-5 to generate 6 candidate questions for each chart, together with their corresponding answers, resulting in a candidate set of 4,038 question-answer

pairs. The candidate set is then manually reviewed. The review contains two levels. The first level checks the quality of the question-answer pair itself. Annotators examine whether the question is clear, whether the answer is correct and unique, and whether the question can be supported by the chart content. The second level checks the interactivity of the question. Annotators examine whether the question can be answered from the initial static chart alone, and whether the answer is hidden in the HTML or underlying data but cannot be obtained through observable interaction. The former cannot reflect dynamic chart understanding, while the latter exceeds the scope of observable interaction. After review, candidate questions are either removed or revised. Questions with low quality, incorrect answers, or insufficient interaction requirements are removed. For charts with meaningful interactivity but imperfect question design, anno-

tators revise the questions and answers so that the required evidence can be obtained through effective interaction. After candidate generation, manual review, and manual revision, we retain 1,440 high-quality question-answer pairs as the official evaluation samples of ChartAct.

**Representative subset construction.** In addition to the full evaluation set, we construct a representative subset of 300 samples for evaluating models with high inference cost. This subset is constructed before evaluating the target models, using the full-set results of 8 models with different scales and access types. We convert the success or failure of these models on each sample into a binary outcome matrix. Based on this matrix, we apply greedy selection followed by local swap search, and finally obtain a subset of 300 samples. This subset substantially reduces the evaluation cost of high-cost models while almost fully preserving the main model performance trends of the full set. The detailed algorithm is provided in the Appendix A.

### 3.2 Environment and Statistics

**Unified interaction environment.** To fairly evaluate different models on dynamic chart tasks, ChartAct reduces the extra variation introduced by runtime platforms and interaction interfaces. We therefore adopt a unified interactive evaluation environment. This environment follows the desktop interaction framework of OSWorld (Xie et al., 2024) and requires all models to complete tasks under the same setting. For each sample, a model observes the current page, performs interaction actions, and submits a final answer after obtaining sufficient evidence. This setting makes the comparison across models mainly reflect their dynamic chart understanding and interactive reasoning abilities. We adapt the original OSWorld runtime to dynamic chart question answering, including task prompts, trajectory turns, and history management. Detailed implementation choices are provided in the Appendix B.

**Dashboard environment.** To better match real use cases of dynamic charts, we further construct dashboard-style page environments. Dynamic charts in real webpages usually appear as data components and form analytical interfaces together with titles and other visual modules. Based on this observation, we use GPT-5.4 to generate diverse dashboard templates covering application scenarios such as finance, industry, law, and medicine. We

then randomly embed the filtered dynamic charts into these templates, so that each chart appears in a concrete page context, which is shown in Figure 2. This environment requires models to first locate the target chart in the page, and then interact with the chart to answer the question. Through this design, ChartAct evaluates dynamic chart understanding in concrete dashboard scenarios.

**Statistics.** Based on the above environment construction, ChartAct contains two paired evaluation environments. Dynamic Chart (DC) provides a clean dynamic chart environment, where the chart is directly displayed on the page. Dashboard Chart (DB) embeds the same dynamic chart into a dashboard page, and is used to evaluate the effect of page context and visual distractors on dynamic chart understanding. The two environments use the same questions and ground-truth answers, allowing paired comparison. ChartAct contains 1,440 question-answer samples, and each sample is instantiated in both DC and DB environments. The source and type distribution of the collected interactive charts is shown in Table 1.

### 3.3 Evaluation

ChartAct adopts an answer-driven evaluation setting. Each evaluation sample contains a question and a ground-truth answer. After observing and interacting with the environment, the model submits a final answer, and the evaluation determines task completion based on this answer. Since answers to dynamic chart questions may involve numbers, text, or natural-language expressions, we use an LLM judge to automatically assess model responses. The judge model determines whether the response is correct according to the question, the ground-truth answer, and the model answer. To reduce the instability of a single judgment, we use multiple votes to obtain the final result. Each sample is finally marked as correct or incorrect. We use success rate as the main evaluation metric and report results by environment type and chart type. The judge prompt, voting setup, and scoring details are provided in the Appendix C.

## 4 Experiments

### 4.1 Experimental Setup

We evaluate current advanced multimodal models and GUI agents on ChartAct. All models use a unified interaction framework, with the same page

Model	Benchmark split				Chart-type score							
	DC	DB	Avg.	Drop	Bar	Line	Pie	Scatter	Box	Heatmap	Other	
<i>Proprietary models</i>												
Claude-Opus-4.7*	<b>85.3</b>	<b>83.7</b>	<b>84.5</b>	1.7	<b>88.7</b>	<b>84.7</b>	<b>91.0</b>	<b>79.2</b>	<b>86.2</b>	<b>75.0</b>	<b>77.8</b>	
GPT-5.5*	65.0	51.7	58.3	13.3	62.9	60.5	54.0	58.3	67.2	43.2	53.7	
Doubao-Seed-2.0-Pro	55.6	39.4	47.5	16.1	53.5	47.3	41.7	49.1	53.3	45.1	37.6	
Gemini-3.1-Pro*	61.0	31.0	46.0	30.0	47.6	47.6	50.0	49.0	46.6	40.9	29.6	
Qwen3.6-Plus	54.7	23.8	39.2	30.8	46.5	36.3	36.2	39.6	45.7	43.2	24.4	
Qwen3-VL-Plus	31.4	13.6	22.5	17.8	26.3	18.6	27.5	22.4	20.3	26.7	12.8	
<i>Open-source models</i>												
Kimi-K2.5	<b>75.3</b>	<b>56.6</b>	<b>66.0</b>	18.8	<b>75.1</b>	<b>62.2</b>	<b>68.0</b>	<b>58.9</b>	<b>72.8</b>	<b>63.1</b>	<b>57.4</b>	
Qwen3.5-122B-A10B	51.9	31.9	41.9	20.0	52.7	41.8	34.1	41.5	45.3	44.7	26.4	
Qwen3.5-35B-A3B	45.7	20.6	33.1	25.1	42.3	29.9	29.3	33.7	34.1	37.4	20.9	
GLM-4.6V	38.7	23.0	30.8	15.7	36.8	25.3	29.8	32.0	33.3	41.3	19.0	
Gemma-4-31B-IT	31.3	14.9	23.1	16.4	26.3	18.7	25.4	22.8	26.1	26.7	16.3	

Table 2: Mixed-scope benchmark results with chart-type subscores. Full-benchmark models are evaluated on all 1,440 Dynamic Chart and 1,440 Dashboard Chart cases. Models marked with \* are evaluated only on the representative subset of 300 cases per benchmark, and those subset scores are used as their benchmark estimates. Chart-type scores pool the two dataset variants. Scores are success rates in percent; bold values indicate the best success rate within each access block.

observations, action interface, task prompts, and answer submission format. ChartAct contains two environments: Dynamic Chart (DC) and Dashboard Chart (DB). DC directly presents the dynamic chart, while DB embeds the same dynamic chart into a dashboard page. The two environments share the same questions and answers, so the performance gap between DC and DB for the same model reflects the additional effect of the dashboard context. For models with high inference cost, we evaluate them on 300 representative samples. This subset has been verified to closely preserve the overall trend, so the corresponding results are used as benchmark estimates and marked with a star in the table. All answers are judged by an LLM judge according to the ground-truth answer and scoring rule. The detailed evaluation criteria are provided in the Appendix.

## 4.2 Main observations

Table 2 provides an overall view of model performance on ChartAct. The results reveal three clear patterns.

**ChartAct remains challenging.** Claude-Opus-4.7 achieves the highest average success rate of 84.5%, but this performance does not appear broadly across other models. Kimi-K2.5 drops to 66.0%, GPT-5.5 reaches 58.3%, and Doubao-Seed-

2.0-Pro and Gemini-3.1-Pro further drop to 47.5% and 46.0%. The clear gap between the best result and the remaining models shows that most models still struggle to understand charts that require interaction.

**Proprietary models show a higher overall ceiling.** Claude-Opus-4.7 ranks first, and GPT-5.5, Doubao-Seed-2.0-Pro, and Gemini-3.1-Pro also fall in the higher range. Among open-source models, the large-scale Kimi-K2.5 performs strongly. Excluding Kimi-K2.5, the best open-source model is Qwen3.5-122B-A10B, with an average success rate of 41.9%. This distribution shows that current dynamic chart understanding ability is more concentrated in stronger models, while open-source models still have substantial room for improvement.

**DB brings a performance drop for all models.** Every model in the table obtains a lower success rate on DB than on DC, showing that dashboard-style page context consistently increases the difficulty of dynamic chart understanding. Claude-Opus-4.7 drops by only 1.7 percentage points, indicating that the strongest model has a better ability to handle page context. Gemini-3.1-Pro and Qwen3.6-Plus drop by 30.0 and 30.8 percentage points, indicating that many models cannot directly

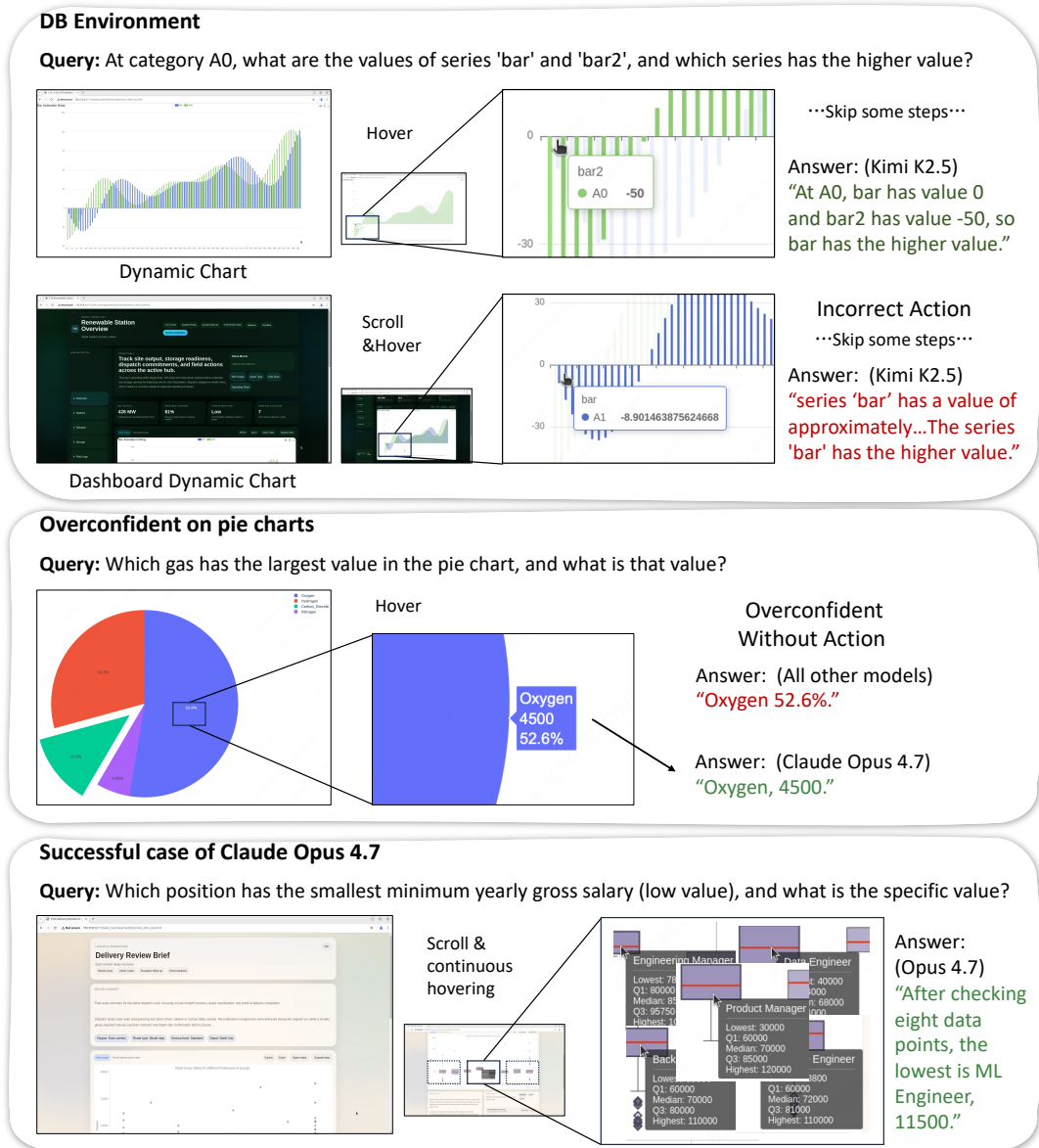


Figure 3: Case studies of model behaviors in ChartAct. The examples show dashboard context causing incorrect interaction, overconfident answering on pie charts without sufficient interaction, and Claude-Opus-4.7 solving a boxplot question through systematic scrolling and continuous hovering.

transfer their ability from clean chart pages to dashboard pages. For models evaluated on the full benchmark, DC and DB use the same charts and questions, so this gap directly reflects the difficulty introduced by the complex page environment. For subset-only models marked with \*, the DC and DB scores are computed on independently selected representative subsets; therefore, their Drop values should be interpreted as numerical estimates of performance degradation rather than strict case-level paired comparisons between each chart and its dashboard counterpart.

### 4.3 Analysis

After splitting the results by chart type, Other obtains the lowest score. This result is intuitive, because Other covers more diverse chart structures, more irregular interaction targets, and a larger search space. Since Other is not a single chart type, we treat it only as a supplementary observation. The main observations are as follows.

**Line has the largest drop from DC to DB.** Line is not the lowest-performing type in the clean environment, but it drops the most after entering the dashboard environment. This change shows that the difficulty of Line is mainly amplified by page

context. Many Line questions require models to trigger the correct tooltip along continuous x-axis positions, while also distinguishing adjacent lines or adjacent data points. Scrolling, resizing, and surrounding components in dashboards increase the complexity of the environment and therefore substantially increase the difficulty of understanding.

**Pie has the smallest drop, but Pie itself is not simple.** Pie already performs relatively low in DC, indicating that its main errors come from inside the chart. Pie lacks regular coordinate axes, and models often ignore interaction and directly estimate or guess the answer. Claude-Opus-4.7 reaches 91.0% on Pie, showing that this task can be solved through effective interaction. Weaker models perform much lower on Pie, further supporting that their errors often come from direct estimation or guessing. The additional DB drop for Pie is small because its data density and environmental complexity are already low.

**Chart types do not form a fixed order.** Claude-Opus-4.7 achieves its highest score on Pie, GPT-5.5 achieves its highest score on Box, and Kimi-K2.5 and Qwen3.5-122B-A10B achieve their highest scores on Bar. This phenomenon shows that the difficulty of dynamic charts cannot be explained only by chart type. Environmental factors such as the position of interaction regions and whether evidence is hidden can change model performance within the same chart type.

#### 4.4 Failure Attribution

Based on the observed error trajectories, model failures can be mainly attributed to three categories.

**Failure to extract evidence.** Some models answer the question directly from the initial screenshot without triggering the interactive state changes of the chart. Although such answers may appear plausible, they often fail on questions that require precise values revealed only through interaction.

**Mis-localized interactions.** The model correctly infers that chart interaction is required, but the cursor is placed on a neighboring data point, an adjacent sector, or an invalid region. This spatial misalignment produces incorrect feedback or no usable feedback, which then leads to an erroneous answer.

**Target object misidentification.** In DB, titles, metric cards, and other visualization components

may appear near the target chart. Some models mistakenly regard these surrounding components as the target chart and continue interacting with the wrong object, causing the subsequent trajectory to deviate from the intended task.

#### 4.5 Case Study

We conduct case studies in Figure 3. The figure shows three representative trajectories.

**Dashboard context changes the interaction trajectory.** The first case compares the same question in DC and DB. In DC, the model directly locates the bar chart and obtains the two series values at A0 by hovering. In DB, the denser page context shifts the interaction to A1, producing a wrong observation and then a wrong answer. This case shows how DB changes the interaction path.

**Pie charts expose overconfident answering.** The second case shows an overconfident error on a pie chart. Most models answer with the visible percentage, Oxygen 52.6%, without observing the true value. Claude-Opus-4.7 hovers over the sector and obtains the correct value, Oxygen 4500. This case shows that pie charts can look simple while still requiring interaction.

**Strong models conduct systematic evidence search.** The third case shows a successful trajectory of Claude-Opus-4.7. The model scrolls to the target boxplot and continuously hovers over multiple boxes. By comparing the observed low values, it identifies ML Engineer with 11500. This case shows the benefit of continuous interaction and evidence comparison.

## 5 Conclusion

We propose ChartAct, a benchmark for dynamic chart understanding. ChartAct requires models to answer chart questions through actions, observations, and reasoning. Experimental results show that current multimodal models and GUI agents still face clear challenges in dynamic chart understanding. Models often fail in interactive evidence acquisition and fine-grained operations. These results show that dynamic charts introduce evaluation requirements beyond static chart understanding. ChartAct provides a new testbed for studying chart understanding in real interactive environments.

## Limitations

ChartAct mainly focuses on dynamic charts from real websites and evaluates them in controllable interactive environments. Although the data covers diverse chart sources and dashboard scenarios, it cannot include all chart libraries and real dashboard layouts. The current evaluation mainly relies on final answers, which measures task completion but cannot fully characterize the quality of intermediate interactions. Future work can further expand chart sources, interaction types, and process-level evaluation.

## References

- Marah Abdin, Sam Ade Jacobs, Ammar Ahmad Awan, Jyoti Aneja, and Ahmed Awadallah et al. 2024. [Phi-3 technical report: A highly capable language model locally on your phone.](#) *arXiv preprint arXiv:2404.14219*, arXiv:2404.14219.
- Saleem Ahmed, Bhavin Jawade, Shubham Pandey, Srirangaraj Setlur, and Venu Govindaraju. 2023. [Realcqa: Scientific chart question answering as a test-bed for first-order logic.](#) In *ICDAR*, pages 14189: 66–83.
- Jinze Bai, Shuai Bai, Shusheng Yang, Shijie Wang, Sinan Tan, Peng Wang, Junyang Lin, Chang Zhou, and Jingren Zhou. 2023. [Qwen-vl: A versatile vision-language model for understanding, localization, text reading, and beyond.](#) *arXiv preprint arXiv:2308.12966*.
- Shuai Bai, Keqin Chen, Xuejing Liu, Jialin Wang, Wenbin Ge, Sibao Song, Kai Dang, and Peng Wang. 2025. [Qwen2.5-vl technical report.](#) *Preprint*, arXiv:2502.13923.
- Ritwick Chaudhry, Sumit Shekhar, Utkarsh Gupta, Pranav Maneriker, Prann Bansal, and Ajay Joshi. 2020. [LEAF-QA: locate, encode & attend for figure question answering.](#) In *IEEE Winter Conference on Applications of Computer Vision, WACV 2020, Snowmass Village, CO, USA, March 1-5, 2020*, pages 3501–3510. IEEE.
- Wentong Chen, Junbo Cui, Jinyi Hu, Yujia Qin, Junjie Fang, Yue Zhao, Chongyi Wang, Jun Liu, Guirong Chen, Yupeng Huo, Yuan Yao, Yankai Lin, Zhiyuan Liu, and Maosong Sun. 2025. [Guicourse: From general vision language model to versatile GUI agent.](#) In *Proceedings of the 63rd Annual Meeting of the Association for Computational Linguistics (Volume 1: Long Papers), ACL 2025, Vienna, Austria, July 27 - August 1, 2025*, pages 21936–21959. Association for Computational Linguistics.
- Zhe Chen, Jiannan Wu, Wenhai Wang, Weijie Su, Guo Chen, Sen Xing, Muyan Zhong, Qinglong Zhang, Xizhou Zhu, Lewei Lu, Bin Li, Ping Luo, Tong Lu, and Yu et al. Qiao. 2023. [Internvl: Scaling up vision foundation models and aligning for generic visual-linguistic tasks.](#) *arXiv preprint arXiv:2312.14238*.
- Zhi-Qi Cheng, Qi Dai, and Alexander G. Hauptmann. 2023. [Chartreader: A unified framework for chart derendering and comprehension without heuristic rules.](#) In *ICCV*, pages 22145–22156.
- Boyu Gou, Ruohan Wang, Boyuan Zheng, Yanan Xie, Cheng Chang, Yiheng Shu, Huan Sun, and Yu Su. 2025. [Navigating the digital world as humans do: Universal visual grounding for GUI agents.](#) In *The Thirteenth International Conference on Learning Representations, ICLR 2025, Singapore, April 24-28, 2025*. OpenReview.net.
- Yucheng Han, Chi Zhang, Xin Chen, Xu Yang, Zhibin Wang, Gang Yu, Bin Fu, and Hanwang Zhang. 2023. [Chartllama: A multimodal LLM for chart understanding and generation.](#) *arXiv preprint arXiv:2311.16483*.
- Muye Huang, Han Lai, Xinyu Zhang, Wenjun Wu, Jie Ma, Lingling Zhang, and Jun Liu. 2025. [Evochart: A benchmark and a self-training approach towards real-world chart understanding.](#) In *AAAI-25, Sponsored by the Association for the Advancement of Artificial Intelligence, February 25 - March 4, 2025, Philadelphia, PA, USA*, pages 3680–3688. AAAI Press.
- Kushal Kafle, Brian L. Price, Scott Cohen, and Christopher Kanan. 2018. [DVQA: understanding data visualizations via question answering.](#) In *CVPR*, pages 5648–5656.
- Samira Ebrahimi Kahou, Vincent Michalski, Adam Atkinson, Ákos Kádár, Adam Trischler, and Yoshua Bengio. 2018. [Figureqa: An annotated figure dataset for visual reasoning.](#) In *ICLR*.
- Aaryaman Kartha, Ahmed Masry, Mohammed Saidul Islam, Thinh Lang, Shadikur Rahman, Ridwan Mahbub, Mizanur Rahman, Mahir Ahmed, Md. Rizwan Parvez, Enamul Hoque, and Shafiq Joty. 2026. [Dashboardqa: Benchmarking multimodal agents for question answering on interactive dashboards.](#) In *Findings of the Association for Computational Linguistics: EACL 2026, Rabat, Morocco, March 24-29, 2026*, Findings of ACL, pages 3385–3407. Association for Computational Linguistics.
- Feng Li, Renrui Zhang, Hao Zhang, Yuanhan Zhang, Bo Li, Wei Li, Zejun Ma, and Chunyuan Li. 2024. [Llava-next-interleave: Tackling multi-image, video, and 3d in large multimodal models.](#) *arXiv preprint arXiv:2407.07895*.
- Fangyu Liu, Julian Martin Eisenschlos, Francesco Piccinno, Syrine Krichene, Chenxi Pang, Kenton Lee, Mandar Joshi, Wenhui Chen, Nigel Collier, and Yasemin Altun. 2023a. [Deplot: One-shot visual language reasoning by plot-to-table translation.](#) *Preprint*, arXiv:2212.10505.
- Fangyu Liu, Francesco Piccinno, Syrine Krichene, Chenxi Pang, Kenton Lee, Mandar Joshi, Yasemin

- Altun, Nigel Collier, and Julian Martin Eisenschlos. 2023b. [Matcha: Enhancing visual language pretraining with math reasoning and chart derendering](#). In *ACL*, pages 12756–12770.
- Yuhang Liu, Pengxiang Li, Zishu Wei, Congkai Xie, Xueyu Hu, Xinchun Xu, Shengyu Zhang, Xiaotian Han, Hongxia Yang, and Fei Wu. 2026. [Infiguiagent: A multimodal generalist GUI agent with native reasoning and reflection](#). In *Proceedings of the 19th Conference of the European Chapter of the Association for Computational Linguistics, EACL 2026 - Volume 1: Long Papers, Rabat, Morocco, March 24-29, 2026*, pages 1035–1051. Association for Computational Linguistics.
- Ahmed Masry, Mohammed Saidul Islam, Mahir Ahmed, Aayush Bajaj, Firoz Kabir, Aaryaman Kartha, Md Tahmid Rahman Laskar, Mizanur Rahman, Shadikur Rahman, Mehrad Shahmohammadi, Megh Thakkar, Md Rizwan Parvez, Enamul Hoque, and Shafiq Joty. 2025. [Chartqapro: A more diverse and challenging benchmark for chart question answering](#). *Preprint*, arXiv:2504.05506.
- Ahmed Masry, Parsa Kavehzadeh, Do Xuan Long, Enamul Hoque, and Shafiq Joty. 2023. [Unichart: A universal vision-language pretrained model for chart comprehension and reasoning](#). In *EMNLP*, pages 14662–14684.
- Ahmed Masry, Do Xuan Long, Jia Qing Tan, Shafiq R. Joty, and Enamul Hoque. 2022. [Chartqa: A benchmark for question answering about charts with visual and logical reasoning](#). In *Findings of ACL*, pages 2263–2279.
- Ahmed Masry, Mehrad Shahmohammadi, Md. Rizwan Parvez, Enamul Hoque, and Shafiq Joty. 2024a. [Chartinstruct: Instruction tuning for chart comprehension and reasoning](#). *arXiv preprint arXiv:2403.09028*.
- Ahmed Masry, Megh Thakkar, Aayush Bajaj, Aaryaman Kartha, Enamul Hoque, and Shafiq Joty. 2024b. [Chartgemma: Visual instruction-tuning for chart reasoning in the wild](#). *Preprint*, arXiv:2407.04172.
- Fanqing Meng, Wenqi Shao, Quanfeng Lu, Peng Gao, Kaipeng Zhang, Yu Qiao, and Ping Luo. 2024. [Chartassisstant: A universal chart multimodal language model via chart-to-table pre-training and multitask instruction tuning](#). *arXiv preprint arXiv: 2401.02384*.
- Nitesh Methani, Pritha Ganguly, Mitesh M. Khapra, and Pratyush Kumar. 2020. [Plotqa: Reasoning over scientific plots](#). In *WACV*, pages 1516–1525.
- Dang Nguyen, Jian Chen, Yu Wang, Gang Wu, Namyong Park, Zhengmian Hu, Hanjia Lyu, Junda Wu, Ryan Aponte, Yu Xia, Xintong Li, Jing Shi, Hongjie Chen, Viet Dac Lai, Zhouhang Xie, Sungchul Kim, Ruiyi Zhang, Tong Yu, Md. Mehrab Tanjim, and 11 others. 2025. [GUI agents: A survey](#). In *Findings of the Association for Computational Linguistics, ACL 2025, Vienna, Austria, July 27 - August 1, 2025*, Findings of ACL, pages 22522–22538. Association for Computational Linguistics.
- Gemma Team, Aishwarya Kamath, Johan Ferret, Shreya Pathak, Nino Vieillard, Ramona Merhej, Sarah Perrin, Tatiana Matejovicova, Alexandre Ramé, Morgane Rivière, Louis Rouillard, and Thomas Mesnard. 2025. [Gemma 3 technical report](#). *Preprint*, arXiv:2503.19786.
- Qwen Team. 2024. [Qvq: To see the world with wisdom](#).
- Peng Wang, Shuai Bai, Sinan Tan, Shijie Wang, Zhihao Fan, Jinze Bai, Keqin Chen, Xuejing Liu, Jialin Wang, Wenbin Ge, Yang Fan, Kai Dang, Mengfei Du, Xuancheng Ren, Rui Men, Dayiheng Liu, Chang Zhou, Jingren Zhou, and Junyang Lin. 2024a. [Qwen2-vl: Enhancing vision-language model’s perception of the world at any resolution](#). *Preprint*, arXiv:2409.12191.
- Zirui Wang, Mengzhou Xia, Luxi He, Howard Chen, Yitao Liu, Richard Zhu, Kaiqu Liang, Xindi Wu, Haotian Liu, Sathika Malladi, Alexis Chevalier, Sanjeev Arora, and Danqi Chen. 2024b. [Charxiv: Charting gaps in realistic chart understanding in multimodal llms](#). *arXiv preprint arXiv:2406.18521*.
- Renqiu Xia, Bo Zhang, Hancheng Ye, Xiangchao Yan, Qi Liu, Hongbin Zhou, Zijun Chen, Min Dou, Botian Shi, Junchi Yan, and Yu Qiao. 2024. [Chartx & chartvlm: A versatile benchmark and foundation model for complicated chart reasoning](#). *CoRR*, abs/2402.12185.
- Tianbao Xie, Danyang Zhang, Jixuan Chen, Xiaochuan Li, Siheng Zhao, Ruisheng Cao, Toh Jing Hua, Zhoujun Cheng, Dongchan Shin, Fangyu Lei, Yitao Liu, Yiheng Xu, Shuyan Zhou, Silvio Savarese, Caiming Xiong, Victor Zhong, and Tao Yu. 2024. [Osworld: Benchmarking multimodal agents for open-ended tasks in real computer environments](#). In *Advances in Neural Information Processing Systems 38: Annual Conference on Neural Information Processing Systems 2024, NeurIPS 2024, Vancouver, BC, Canada, December 10 - 15, 2024*.
- Zhengzhuo Xu, Bowen Qu, Yiyan Qi, Sinan Du, Chengjin Xu, Chun Yuan, and Jian Guo. 2025. [Chartmoe: Mixture of diversely aligned expert connector for chart understanding](#). *Preprint*, arXiv:2409.03277.
- Jianwei Yang, Hao Zhang, Feng Li, Xueyan Zou, Chunyuan Li, and Jianfeng Gao. 2023. [Set-of-mark prompting unleashes extraordinary visual grounding in GPT-4V](#). *CoRR*, abs/2310.11441.
- Leyang Yang, Ziwei Wang, Xiaoxuan Tang, Sheng Zhou, Dajun Chen, Wei Jiang, and Yong Li. 2026. [Probench: Benchmarking GUI agents with accurate process information](#). In *Fortieth AAI Conference on Artificial Intelligence, Thirty-Eighth Conference on Innovative Applications of Artificial Intelligence, Sixteenth Symposium on Educational Advances in Artificial Intelligence, AAI 2026, Singapore, January 20-27, 2026*, pages 27547–27555. AAI Press.

Jiabo Ye, Xi Zhang, Haiyang Xu, Haowei Liu, Junyang Wang, Zhaoqing Zhu, Ziwei Zheng, Feiyu Gao, Junjie Cao, Zhengxi Lu, Jitong Liao, Qi Zheng, Fei Huang, Jingren Zhou, and Ming Yan. 2025. [Mobile-agent-v3: Fundamental agents for GUI automation](#). *CoRR*, abs/2508.15144.

Liang Zhang, Anwen Hu, Haiyang Xu, Ming Yan, Yichen Xu, Qin Jin, Ji Zhang, and Fei Huang. 2024. [Tinychart: Efficient chart understanding with visual token merging and program-of-thoughts learning](#). *arXiv preprint arXiv: 2404.16635*.

## A Representative Subset Construction

This appendix describes how we construct the 300-case representative subsets used for high-cost model evaluation. ChartAct contains two benchmark variants, Dynamic Chart (DC) and Dashboard Chart (DB). Each variant contains 1,440 cases. Evaluating every high-cost model on all  $2 \times 1440$  cases is expensive, so we construct one 300-case subset for DC and one 300-case subset for DB. The two subsets are selected independently, but they are generated using the same selection algorithm and the same objective design. Importantly, the target high-cost models are not involved in subset construction. The subsets are constructed only from the full-set results of eight lower-cost pilot models. Specifically, the eight pilot models are Doubao-Seed-2.0-Pro, Kimi-K2.5, Qwen3.6-Plus, Qwen3-VL-Plus, Gemma-4-31B-IT, GLM-4.6V, Qwen3.5-122B-A10B, and Qwen3.5-35B-A3B. The subset-only high-cost models are excluded from this construction process to avoid using their evaluation outcomes during subset selection.

### A.1 Pilot Outcome Matrix

For each benchmark variant, we first collect the full-set binary results of the eight pilot models. Let  $D = \{x_i\}_{i=1}^N$  denote one full benchmark variant, where  $N = 1440$ , and let  $M = 8$  be the number of pilot models. We construct a binary outcome matrix

$$Y \in \{0, 1\}^{N \times M},$$

where  $Y_{ij} = 1$  means that pilot model  $j$  correctly solves case  $x_i$ , and  $Y_{ij} = 0$  otherwise. Each row of  $Y$  therefore summarizes how the eight pilot models behave on one case.

From this matrix, each case receives two types of calibration information. The first is its empirical difficulty,

$$d_i = \sum_{j=1}^M Y_{ij},$$

which is the number of pilot models that solve the case. A case with  $d_i = 8$  is easy for all pilot models, while a case with  $d_i = 0$  is difficult for all pilot models. Intermediate values indicate cases that separate the pilot models. The second is the chart type of the case, such as line, bar, pie, scatter, heatmap, box, or other. These features allow the subset selection process to preserve both performance behavior and content coverage.

### A.2 Representativeness Objective

The goal is to select a subset  $S \subset D$  with  $|S| = 300$  such that  $S$  behaves as similarly as possible to the full benchmark  $D$ . We define a weighted representativeness objective with four terms:

$$\mathcal{L}(S) = 5.0 \Delta_{\text{acc}}(S, D) + 2.0 \Delta_{\text{gap}}(S, D) + 2.0 \Delta_{\text{diff}}(S, D) + 1.2 \Delta_{\text{type}}(S, D).$$

Lower values of  $\mathcal{L}(S)$  indicate a more representative subset.

**Model accuracy deviation.** For pilot model  $j$ , let

$$a_j(S) = \frac{1}{|S|} \sum_{x_i \in S} Y_{ij}$$

be its accuracy on subset  $S$ , and define  $a_j(D)$  analogously on the full benchmark. The model-accuracy deviation is

$$\Delta_{\text{acc}}(S, D) = \frac{1}{M} \sum_{j=1}^M |a_j(S) - a_j(D)|.$$

This term makes the selected subset preserve the absolute performance level of each pilot model.

**Pairwise model-gap deviation.** Matching only individual accuracies is not sufficient; the subset should also preserve the relative gaps between models. For each pair of pilot models  $(u, v)$ , define the accuracy gap on subset  $S$  as

$$g_{uv}(S) = a_u(S) - a_v(S).$$

The pairwise-gap deviation is

$$\Delta_{\text{gap}}(S, D) = \frac{1}{\binom{M}{2}} \sum_{1 \leq u < v \leq M} |g_{uv}(S) - g_{uv}(D)|.$$

This term encourages the subset to preserve the model ordering and the relative separation between pilot models.

**Difficulty-distribution deviation.** Let  $p_b^{\text{diff}}(S)$  be the proportion of cases in  $S$  whose difficulty is  $b$ , where  $b \in \{0, 1, \dots, 8\}$ . The difficulty-distribution deviation is

$$\Delta_{\text{diff}}(S, D) = \sum_{b=0}^8 \left| p_b^{\text{diff}}(S) - p_b^{\text{diff}}(D) \right|.$$

This term prevents the subset from becoming systematically easier or harder than the full benchmark.

**Chart-type distribution deviation.** Let  $p_t^{\text{type}}(S)$  be the proportion of cases in  $S$  with chart type  $t$ . The chart-type distribution deviation is

$$\Delta_{\text{type}}(S, D) = \sum_t \left| p_t^{\text{type}}(S) - p_t^{\text{type}}(D) \right|.$$

This term preserves the content composition of the full benchmark across major chart categories.

### A.3 Greedy Construction

After defining the objective, we search for a low-score subset using greedy construction followed by local swap search. For each benchmark variant, the algorithm starts with an empty selected set  $S = \emptyset$  and an available pool  $U = D$ . It then repeatedly adds one case until  $|S| = 300$ .

At greedy step  $k$ , where  $0 \leq k < 300$ , the algorithm evaluates every currently unselected candidate case  $x \in U$ . For each candidate, it temporarily forms

$$S_x = S \cup \{x\}$$

and computes the objective value  $\mathcal{L}(S_x)$ . All candidate cases are then ranked by this score in ascending order. The lowest-score candidates are the cases that make the current subset most similar to the full benchmark after being added.

To avoid a brittle deterministic path, we do not always select only the single best candidate. Instead, we take the top  $K_{\text{top}} = 8$  candidates and sample one candidate from them using rank-based probabilities. If a candidate is ranked  $r$  among the top candidates, its sampling weight is

$$w_r = \frac{1}{r}.$$

Thus, the best candidate has the largest probability, but lower-ranked candidates among the top eight can still be selected. This small amount of randomness reduces the risk that an early greedy choice traps the search in an inferior local solution. We

use a fixed random seed for reproducibility. The DC subset uses seed 20260521, and the DB subset uses seed 20261521.

The greedy stage can be summarized as follows:

1. Initialize  $S = \emptyset$ .
2. For every unselected case  $x$ , compute  $\mathcal{L}(S \cup \{x\})$ .
3. Rank all candidates by this objective value.
4. Sample one case from the top eight candidates with probability proportional to  $1/r$ , where  $r$  is the candidate rank.
5. Add the sampled case to  $S$ .
6. Repeat until  $|S| = 300$ .

### A.4 Local Swap Search

The greedy stage constructs a strong initial subset, but greedy selection only optimizes the immediate next addition. A case selected early may become suboptimal after many later additions. To further improve the subset, we apply a local swap search after the greedy subset reaches 300 cases.

Let  $S$  be the current 300-case subset and let  $D \setminus S$  be the set of unselected cases. At each local-search iteration, the algorithm randomly selects one case  $x_{\text{out}} \in S$  and one case  $x_{\text{in}} \in D \setminus S$ . It proposes a swapped subset

$$S' = (S \setminus \{x_{\text{out}}\}) \cup \{x_{\text{in}}\}.$$

The swap is accepted only if it strictly reduces the representativeness objective:

$$\mathcal{L}(S') < \mathcal{L}(S).$$

If the objective does not improve, the swap is rejected and the algorithm keeps the original subset. Therefore, the local-search stage monotonically decreases the objective value over accepted moves.

In our implementation, the local search runs for at most 25,000 swap trials for each benchmark variant. We also use an early stopping rule: if the search encounters 5,000 consecutive non-improving swap proposals, it stops early. The output of this stage is a locally optimized 300-case subset.

## A.5 Final Subsets and Validation

We run the above procedure independently for DC and DB. This produces two 300-case subsets, one for each benchmark variant. The resulting subsets reduce the number of evaluated cases from  $2 \times 1440$  to  $2 \times 300$ , reducing the evaluation load by approximately 79.2%.

We validate the selected subsets by comparing pilot-model performance on the 300-case subsets against performance on the corresponding full 1,440-case benchmarks. For DC, the mean absolute pilot-model accuracy error is 0.000590 and the maximum absolute accuracy error is 0.002083. For DB, the mean absolute pilot-model accuracy error is 0.001267 and the maximum absolute accuracy error is 0.002222. In both benchmark variants, the pilot-model ranking is preserved exactly, with zero rank inversions. These results indicate that the selected subsets closely preserve the evaluation behavior of the full benchmark while substantially reducing evaluation cost.

## B Implementation Details and Experimental Settings

This appendix summarizes the implementation changes we made on top of the original OSWorld-style evaluation framework and the hyperparameters used in our experiments. The goal of these changes is to adapt the desktop automation runtime to answer-driven dynamic chart understanding while keeping the interaction interface as consistent as possible across models.

### B.1 Incremental Changes over OSWorld

Our runtime follows the basic OSWorld design: each task is executed in a virtualized Ubuntu desktop, the agent observes the current screen, emits GUI actions, and the environment executes those actions before returning the next observation. We make several task-specific modifications for ChartAct.

**Chart-specific prompting.** We replace the generic desktop-task prompt with a chart-focused prompt in `mm_agents/prompts.py`. The main prompt explicitly defines the task as interacting with charts already displayed in a browser, collecting information from chart states, and answering chart-related questions. In particular, models are not allowed to use developer tools, inspect page source, call screenshot APIs, or rely on hidden

### Core excerpt of the ChartAct interaction prompt

Task: interact with charts already displayed on a webpage to collect information and answer chart-related questions.

Use only normal browser interactions. Do not use developer mode or access the webpage source code.

Case 1: Perform an Interaction. Return Python code in exactly one code block. Do not use `pyautogui.locateCenterOnScreen` or `pyautogui.screenshot()`.

Case 2: Answer the Question. Return `FINAL_JSON: {"Answer": "you fill your answer here"}`.

If `CURRENT_STEP` equals `MAX_STEPS`, do not output Python code; output the final answer instead.

Figure 4: Core excerpt of the modified interaction prompt used in the main framework.

webpage metadata. Figure 4 shows the core excerpt of the modified interaction prompt used in the main framework.

**Answer-driven termination.** The original OSWorld tasks are often evaluated through the final desktop state. In ChartAct, each task is a question-answering problem. We therefore add a machine-readable final-answer channel:

```
FINAL_JSON: {"Answer": "..."}.
```

During evaluation, `lib_run_single.py` extracts this field, writes it to `final_answer.txt`, and stores it in `env.agent_answer`. The environment evaluator then grades this submitted answer rather than treating a generic DONE action as sufficient.

**Step-aware interaction control.** We modify the agent wrapper in `mm_agents/agent.py` to pass the current step index into the prompt. When the maximum step budget is reached, the prompt explicitly forbids further Python actions and requires the model to submit its best final answer. This prevents models from spending the final turn on an action for which no follow-up observation will be available.

**Unified model routing.** We extend the model-calling code in `mm_agents/agent.py` so that the main evaluation framework routes different model families through a common OpenAI-compatible chat-completion interface whenever possible. The routing layer normalizes provider-specific base URLs, API keys, token fields, and reasoning/thinking options, while preserving the

same visible task prompt, screenshot input, action grammar, history window, and final-answer format for the main comparison.

**Execution safety and logging.** The environment executes interaction actions through the `pyautogui` action space. Before execution, generated Python commands are sanitized to remove non-GUI or dangerous statements. For each task, the runner stores the initial screenshot, per-step screenshots, structured trajectory logs, the final answer, a screen recording, and the scalar result. These artifacts make the evaluation auditable and allow later error analysis without rerunning the interaction.

## B.2 Shared Evaluation Parameters

Table 3 lists the parameters kept fixed in the main fair-comparison framework. We do not manually set the internal context length of each proprietary model. Instead, we control the agent-side context window by keeping at most the latest seven trajectory turns in the prompt. The maximum model output length is fixed to 3,000 tokens for all reported runs.

The dataset selector is changed according to the evaluated benchmark split. For full-set experiments, the metadata files are `chartall.json` for Dynamic Chart and `webchartall.json` for Dashboard Chart. For cost-controlled evaluation, the same framework is run on the representative subset metadata files, such as `chart_300.json` and `webchart_300.json`. These metadata choices select the task pool; they do not alter the interaction interface or model-facing prompt.

## B.3 Model-Specific Interface Settings

The experiments involve eight reported model entries, all evaluated with the same main interaction framework. Table 4 summarizes the model-specific interface settings used by the unified routing layer.

## C LLM Judge Grading Protocol

ChartAct uses answer-driven grading. Each task stores a question, a reference answer, and a rubric in the task JSON. After the agent submits `FINAL_JSON`, the evaluator retrieves the cached `Answer` field through the `agent_answer` getter and passes it to `llm_judge`. Missing or empty answers are directly assigned score 0.0.

## C.1 Judge Model and Voting Setup

We use `deepseek-v4-pro` as the LLM judge. The judge is called through the DeepSeek API endpoint `https://api.deepseek.com`. The judge configuration uses three independent votes and an acceptance threshold of two votes. In other words, a task is marked correct only if at least two of the three judge calls return a positive decision. The judge decoding temperature is set to 0.0, the maximum output length is 1,024 tokens, the timeout is 45 seconds, and each vote allows one retry with a two-second retry backoff. We set the judge reasoning effort to low and enable the provider-side thinking mode. API keys are loaded from the local judge configuration file and are not included in the paper.

## C.2 Judge Prompt

For each vote, the judge receives a system message and a user message. The system message enforces binary scoring, while the user message provides the task question, the ground-truth answer, the agent answer, and the task-specific rubric. The complete prompt template is shown in Figure 5. The placeholders are filled from the task JSON and the submitted agent answer.

## C.3 Score Aggregation and Regrading

The judge output parser extracts the first valid binary score, either 1.0 or 0.0. Since the judge output is binary, a parsed score of 1.0 is counted as a passing vote, while a parsed score of 0.0 is counted as a failing vote. Let  $v$  be the number of passing votes among the three judge calls. The final task score is

$$\text{score} = \begin{cases} 1.0, & v \geq 2, \\ 0.0, & v < 2. \end{cases}$$

The benchmark success rate is the mean of these binary task scores.

We also design an offline grading script for post-hoc evaluation after the interaction trajectories have been completed. The script scans existing result directories, reloads each task configuration, reads the saved `final_answer.txt`, reruns the current `llm_judge`, and optionally updates the stored grading result. Thus, if the judge model, voting configuration, or rubric is updated, we can recompute scores from saved answers without rerunning the expensive GUI interaction trajectories.

Parameter	Setting
Main runner	run_multienv.py
Main agent wrapper	PromptAgent in mm_agents/agent.py
Environment provider	Docker-based OSWorld desktop environment
Operating system and browser	Ubuntu desktop with Google Chrome opened to the target chart page
Screen resolution	1920 × 1080
Observation type	Screenshot-only input in the reported main setting
Action space	pyautogui desktop-control code
Maximum interaction budget	15 effective environment steps per task
Agent-side history window	Last 7 trajectory turns (max_trajectory_length=7)
Post-action wait	1.0 second after each executed action
Sampling temperature	0.3
Top- $p$	0.9
Maximum output tokens	3,000 tokens per model call
Final-answer format	FINAL_JSON: {"Answer": "..."} results/pyautogui/screenshot/<model>/...
Result directory format	results/pyautogui/screenshot/<model>/...
Evaluation metric	Answer-based llm_judge with configurable majority voting
Parallel environments	Varied only for throughput according to API and machine capacity; this does not change the per-task protocol

Table 3: Shared experimental settings used by the main fair-comparison framework. The number of parallel environments is varied only for throughput and does not change the per-task interaction protocol.

Model entry	Model-specific interface setting
<i>Full benchmark: 2 × 1440 cases</i>	
doubao-seed-2-0-pro-260215	Seed/Doubao OpenAI-compatible route; reasoning depth set to high.
kimi-k2.5	Kimi OpenAI-compatible route; Kimi thinking switch set to disabled.
qwen3.6-plus	Qwen OpenAI-compatible route; Qwen thinking-token budget set to 1000 in the recorded run.
qwen3-v1-plus	Qwen OpenAI-compatible route; DashScope thinking enabled with thinking budget 2100.
gemma-4-31b-it	Open-weight model served through the unified OpenAI-compatible route; no extra reasoning switch.
glm-4.6v	Open-weight GLM route; response postprocessing removes reasoning tags before action parsing.
qwen3.5-122b-a10b	Open-weight Qwen route; Qwen thinking-token budget set to 2100.
qwen3.5-35b-a3b	Open-weight Qwen route; Qwen thinking-token budget set to 1500 in the recorded run.
<i>Representative subset: 2 × 300 cases</i>	
claude-opus-4-7	Claude OpenAI-compatible route; unsupported sampling parameters are removed by the routing layer.
gpt-5.5	GPT OpenAI-compatible route; GPT-5 payload uses max_completion_tokens for the 3,000-token output cap.
gemini-3.1-pro-preview	Gemini OpenAI-compatible route; Gemini thinking depth set to low through provider-specific thinking configuration.

Table 4: Reported model entries and model-specific interface settings. Full and subset entries use the same main wrapper, prompt, action space, history window, step budget, answer format, and grading protocol; subset entries are evaluated on the representative 300-case split for each benchmark variant.

**System message**  
You are a strict judge. Output ONLY 1.0 or 0.0.

**User message**  
[Task Question]  
{question}  
[Ground Truth / Expected]  
{expected}  
[Agent's Actual Answer]  
{extracted\_answer}

Based on the task question and the ground-truth answer, is the Agent's answer correct?  
Output 1.0 for Yes, 0.0 for No.  
When you compare answers, focus on the actual correctness of the answers rather than wording or language.  
If the meaning of the answer is the same as the standard answer, give full marks.  
For numerical questions, rounding is allowed when the precision remains reasonable.

Figure 5: Effective prompt template used by the LLM judge for ChartAct grading.